LBL--23623

DE87 012876

THE LBL 1-2 GEV SYNCHROTRON RADIATION SOURCE*

Frank B. Selph for the Light Source Design Group

Lawrence Berkeley Laboratory
University of California
Berkeley, CA 94720

June 1987

*This was supported by the Director, Office of Energy Research, Office of High Energy and Nuclear Physics, High Energy Physics Division, U.S. Dept. of Energy, under Contract No. DE-AC03-76SF00098.

THE LBL 1-2 GEV SYNCHROTRON RADIATION SOURCE*

Frank. B. SELPH for the Light Source Design Group

Lawrence Berkeley Laboratory, University of California, Berkeley, CA 94720

ABSTRACT

The design of the 1-2 GeV Synchrotron Radiation Source to be built at the Lawrence Berkeley Laboratory is described. The goal of this facility is to provide very high brightness photon beams in the ultraviolet and soft X-ray regions. The photon energy range to be served is from 0.5 eV to 10 keV, with the brightest beams available in the 1 eV - 1 keV interval. For time-resolved experiments, beam pulses of a few tens of picoseconds will be available. Emphasis will be on the use of undulators and wigglers to produce high quality, intense beams. Initially, four of the former and one of the latter devices will be installed, with six long straight sections left open for future installations. In addition, provision is being made for 48 beamlines from bending magnets.

The storage ring is optimized for operation at 1.5 GeV, with a maximum energy of 1.9 GeV. The injection system includes a 1.5 GeV booster synchrotron for full energy injection at the nominal operating energy of the storage ring. Filling time for the maximum storage ring intensity of 400 mA is about 2 minutes, and beam lifetime will be about 6 hours. Attention has been given to the extraordinary requirements for beam stability, and to the need to independently control photon beam alignment. Typical rms beam size in insertion regions is 201 μm horizontal, and 38 μm vertical.

The manner in which this design achieves very high spectral brightness from undulators and wigglers, while maintaining a modest value for the beam current, will be described. Primarily, this requires that the design of the lattice, the arrangement of bending magnets, focusing quadrupoles and straight sections, be done with this in mind.

A very good vacuum (10^{-9} Torr) is required ; this is achieved with the aid of a novel design of vacuum chamber that minimizes the effects of outgassing. Means must also be provided for avoiding instabilities that would cause growth of the storage ring beam size.

Description of the Facility

The 1-2 GeV Synchrotron Radiation Source will be located at Lawrence Berkeley Laboratory, on the site of the 184-Inch Cyclotron. The Cyclotron will be shut down and dismantled as part of the Light Source project. An extension to the existing cyclotron building will be added, to house the new storage ring facilities, photon beamlines and experimental areas. A plan of the overall layout is shown in Fig. 1. As is shown in the figure, beamlines will be installed for only part of the ring, leaving the remainder for future additions. Figure 2 shows a cross section of the storage ring enclosure. The construction began in the fall of 1986, and will be complete in 6 years, in 1992. The cost is $98.7 M. A full description of the facility, including construction schedule and costs, will be found in the Conceptual Design Report [1].

The principal parameters of the storage ring are shown in Table I. The storage ring circumference is 197.8 m, with 12 straight sections, 11 of which are available for insertion devices. The total space made available for insertion devices is 55 m, more than one-quarter of the 197 m circumference. The injector complex, consisting of a 50 MeV electron linac and a 1.5 GeV booster synchrotron, is located inside the storage ring, as shown in Fig. 3. Filling time required to achieve the design current of 400 mA will be short, about 2 minutes. The very small natural beam emittance of 4.1×10^{-9} πm-rad will permit photon beams of exceptional brightness. Two modes of operation are foreseen -- a multibunch mode in which about three-quarters of the storage ring is filled (leaving a gap for ion clearing purposes), and a single-bunch mode, in which one, or at most a few, bunches are injected into the storage ring. The half-life

of the stored beam, in the worst case, with a single-bunch mode and operating with a 1 cm vacuum gap, is 5 hours. For multibunch operation the half-life should be longer, about 7 hours. Good transfer efficiency is maintained in the booster by using single turn injection and extraction. A FODO lattice is used for the booster, with straight sections for injection, extraction and rf cavities being obtained by leaving out some dipoles, creating four superperiods in the lattice.

The performance goals of the Light Source (Table II) were developed by a consensus of the user community, and confirmed in a Workshop held at Berkeley in 1985 [2]. As mentioned above, there will be an initial complement of five insertion devices in the storage ring, with space for future addition of six more. Tentative parameters for the first five devices, four undulators and one wiggler, are given in Table III. Some characteristics of the radiation from these devices is given in Figs. 4-6. Spectral brightness is shown in Fig. 4, photon flux in Fig. 5, and average coherent power in Fig. 6, as a function of photon energy. Each period of the storage ring, with a straight section for an insertion device and the following three bend magnets, will serve a family of beamlines, as shown in Fig. 7. One line emanates from the insertion device, and four other lines accept beam from the bending magnets. Any of the latter lines can be split to serve two or more users.

Lattice Design Considerations

The design of the storage ring lattice, i.e., the arrangement of dipole, quadrupole and sextupole magnets, is of great importance in determining the beam quality, and the usability of the facility. The most important requirements to be satisfied in the design are the following:

- Availability of many long straight sections for insertion devices.

- An adequate tuning range for betatron oscillation frequencies in both transverse planes, in order to avoid resonances and instabilities.

- A need for short bunches -- tens of picoseconds.

- An adequate dynamic aperture (i.e., the aperture over which electrons have stable oscillations).

- A large momentum acceptance, in order to maximize electron beam lifetime due to large-angle intrabeam scattering (the Touschek effect).

A thorough study was undertaken of a number of lattice options to determine the lattice that would most completely satisfy these requirements. The so-called TBA, or triple-bend achromat, lattice was chosen as having the best properties [3]. One cell of this structure is shown in Fig. 8; the corresponding lattice functions are shown in Fig. 9. The bending magnets are combined-function, with a magnet gradient which focuses vertically. Betatron functions in the long straight sections are controlled by the quadrupoles labeled QF and QD in Fig. 8, and the dispersion in the center of the arc is controlled with the quadruploles labeled QFA.

The natural chromaticity of the lattice (the change in betatron frequency with momentum deviation) is negative. If uncorrected, this will cause the beam to become unstable due to an effect called the head-tail instability. Two families of sextupoles (SD and SF) are used to control the chromaticity and make it zero or slightly positive. The sextupoles, however, introduce nonlinearities into the electron motion and the betatron tune becomes amplitude dependent. This reduces the aperture within which the electron motion is stable, called the dynamic aperture. Additionally, higher order multipole fields within the lattice magnets, caused mainly by finite construction tolerances, lead to an increase in the amplitude dependence and to a reduction in the dynamic aperture, as shown in Fig. 10. The outer solid line shows the aperture resulting

from the effects of the chromaticity sextupoles. The inner shaded band shows the reduction in aperture when realistic construction tolerances are taken into account.

Collective Effects

Collective interactions, both between beam bunches and between the beam and its environment, influence the beam lifetime, the beam transverse dimensions, and the minimum beam bunch length that can be achieved. The bunch length, as a function of beam current, depends upon the broadband impedance of the vacuum chamber. This has been estimated to be about 2.5 ohms. Some measurements which were done on the SPEAR ring, however, have shown empirically that the impedance seen by the beam decreases for bunch lengths shorter than the beam pipe radius [5]. Calculated bunch lengths are shown as a function of beam current for the single-bunch case in Fig. 11a, and for the multibunch case in Fig. 11b. In each case, the use of SPEAR scaling is shown, as well as the more pessimistic result of assuming no impedance roll-off for short bunch lengths. These results show that, if the impedance decreases as expected for short bunches, bunch lengths as short as 30 ps can be achieved even at high beam current.

To insure stable operation, instabilities that could cause beam jitter or beam loss have been carefully studied, using a computer code called ZAP [6]. A careful analysis of this problem, which is given in Ref. [1], concludes that, without some preventive measures, a number of resonance modes would have growth times considerably shorter than the synchrotron radiation damping times. Careful design of the rf cavities to reduce or eliminate parasitic high-order modes is thus necessary to minimize or avoid the excitation of longitudinal and transverse coupled-bunch instabilities. In addition, active mode supression (feedback) will be employed as necessary to supress coupled-bunch instabilities. The kicker voltages and bandwidth required for the feedback system are moderate.

An important goal of the design is to achieve an electron beam half-life of many hours. Beam lifetime is dependent upon reducing losses due to gas scattering and large angle intrabeam scattering (the Touschek effect). The first is achieved by maintaining a low pressure of 10^{-9} Torr (see below). The dominant gas scattering loss occurs at the regions of smallest aperture; these will be at the undulator gaps, which can be as small as 1 cm. For the second, the rf voltage must be high enough to provide momentum acceptance of 3.5%, which will assure a high Touschek lifetime. To provide the short bunches, an rf frequency of 500 MHz was chosen. The predicted beam lifetimes, obtained with the ZAP code, with all of these effects taken into account, are shown in Fig. 12.

Ion Trapping

Residual gas molecules are ionized by the electron beam. If they become trapped in the potential well created by the electrons, beam lifetime can be reduced and beam size can increase, reducing the brightness of the photon beam.

The method adopted for avoiding ion trapping is to maintain a gap in the circulating beam, leaving contiguous rf buckets unfilled for about one-quarter of the circumference. This technique has been used successfully at a number of operating storage rings [7]. In order to understand how effective this measure would be for our design, the ion motion within the potential well of the beam was simulated, both with and without a beam gap [4]. It was found that, without the gap, all ion masses of interest would be stable, i.e., could remain in the electron beam, whereas the introduction of a substantial gap caused most ion masses to become unstable, i.e., to leave the electron beam. Some of these results are shown in Fig. 13.

Magnets and Vacuum

Several types of magnets are to be fabricated for the Light Source project:

- Gradient bending magnets, which both bend and focus the beam.
- Quadrupole magnets to focus the beam.
- Sextupole magnets for chromaticity correction.
- Skew quadrupoles to control vertical beam size.
- Small dipole magnets for vertical and horizontal steering.
- Septum magnets for booster injection and extraction, and storage ring injection.
- Kicker magnets for booster injection and extraction.
- Bump magnets for moving the storage ring orbit close to the septum.
- Solenoid magnets for focusing the beam form the source through the 50 MeV linac.

Existing storage ring technology is adequate to meet the requirements for fabrication tolerances and placement accuracy. For the storage ring, the required tolerances are readily achieved that will satisfy dynamic aperture requirements. The storage ring magnet yokes are designed with a C configuration to accommodate the novel vacuum chamber, which extends outside the ring. The combined function bending magnets are shown in cross section in Fig. 14. A quadrupole magnet cross section is shown in Fig. 15. The yokes are formed in two halves, and keyed to achieve the desired precision in assembly.

The vacuum chamber must maintain a pressure of 1×10^{-9} Torr in the vicinity of the electron beam. In order to accomplish this, we must be able to pump efficiently the large amount of gas released by synchrotron radiation striking the chamber walls. The novel solution adopted is illustrated in Fig. 16. The outer wall of the chamber enclosing the circulating beam contains a 1 cm high slot, which opens to a much larger outer chamber. The synchrotron radiation passes through this slot, and strikes a water cooled photon stop in the outer chamber. Directly beneath each stop is a titanium sublimation pump. In order to achieve the complex shapes and precise tolerances required, as well as strength where needed, the vacuum chamber is machined from aluminum alloy.

Injection System

In order to achieve the electron beam quality and reliability of operation expected in the storage ring, a 1 Hz booster synchrotron injecting at full energy is used. This in turn is injected with a 50 MeV electron linac. Table IV lists the performance characteristics of this injector facility. Table V shows the expected transmitted intensities of electrons, from the gun to the storage ring, for the two operating modes. In order to achieve a relatively high linac current, while keeping the peak current of the electron gun at modest values, subharmonic bunching is used between the gun and linac. The design is similar to that used at SLAC for the SLC injector [8].

In the single-bunch mode, the gun must deliver 2.4 A with a pulse duration of 2.5 ns. Two subharmonic buncher cavities located between the gun and linac compress this pulse so that it can be accepted by the S-band buncher at the entrance to the linac, and accelerated in the linac. The multibunch mode of operation is similar, except that a lower gun current of 1 A, with a pulse length of 100 ns, is sufficient to produce a train of 17 linac pulses for injection into the booster. In order to insure that the beam energy spread is not increased by rf phase mismatch between systems, the subharmonic

buncher, linac and booster are phase-locked. The relation between the beam bunches and the rf in these systems is shown in Fig. 17.

The linac is a 4 m, disk-loaded waveguide structure, operated in a traveling-wave mode. At its entrance a short (0.105 m) S-band buncher is used, operating at the linac frequency of 2998 MHz. The linac structure is divided into two 2-m sections, each with a klystron driver and load. This arrangement provides flexibility in tuning linac phases, which is helpful in dealing with beam loading, and also reduces the power required from a single klystron, enhancing reliability.

The booster synchrotron, operating at 1 Hz, is used to accelerate the 50 MeV beam from the linac to the nominal storage ring operating energy of 1.5 GeV. Single-turn injection and extraction are used to insure good overall injection efficiency for the booster. The booster lattice is a simple FODO separated-function structure, with some bending magnets omitted to provide straight sections for injection, extraction , and rf cavities (see Fig. 3). Two sextupole families are used to correct chromaticity throughout the acceleration cycle. Families of steering magnets are used for orbit correction, but the requirements are less severe than for the storage ring. Further details of the injection system design can be found in Ref. [9].

Instrumentation and Control Systems

Diagnostic instrumentation is used to control and measure electron beam position, emittance, momentum spread, intensity and bunch length to the accuracy needed to meet design specifications for the stored electron beam. In the storage ring, 96 beam position monitors (BPMs) capable of a position accuracy on the order of 0.03 mm are used [10]. The design of the BPM is illustrated in Fig. 18. Flush mounting of the button pickups in the vacuum chamber wall ensures that the electromagnetic disturbance to the circulating beam from the BPMs is kept to a minimum. Each button has its own local processing electronics, with information transmitted digitally to the control

room. Fast single-turn measurements are accurate to a few percent; for stored beam measurements, many turns are averaged to achieve greater accuracy. Other storage ring instrumentation includes synchrotron light optical monitors to measure beam transverse dimensions and bunch length, and a current transformer to measure intensity. Similar instrumentation is used in the booster.

In the transport between the linac and booster, and between the booster and storage ring, the instrumentation, in addition to BPMs, includes intensity monitors, adjustable collimators, and scintillation screens viewed with TV monitors. In the linac to booster line, at a point where a focal condition exists but where dispersion is high, the momentum spread can be measured and the source and linac can be tuned to minimize the spread. Collimators at that point are employed to control the momentum spread of the beam injected into the booster.

The computer control system uses a microprocessor-based architecture that permits a distributed database, parallel processing, and rapid collection and transmission of data. Figure 19 is a schematic of the major elements of the control system. Analog data are collected, digitized, subjected to a certain amount of processing, and stored in the components labeled ILC (for intelligent local controller) and IOMM (input-output micro-module). A copy of this data is transmitted over fiber optic links to the CMM (collector micro-module), which functions as a central repository for data. This data is accessed, asynchronously, by the DMM (display micro-module), which is an interface to the operator consoles, and through Ethernet, to development workstations and other computer systems. Control of insertion devices by users will be possible from consoles located near the experiment. Operator commands, and other changes to the database, flow from the DMM back through the CMM to the front-end ILC and IOMM modules. Data security will be implemented by a scheme in which data can be read by any console but changes to data can only be made by authorization of the chief operator.

The DMM contains several processors, linked by an internal bus that is separate from the input-output ports by which data is received and transmitted outside the DMM. The CMM contains several dual-ported processors, allowing receipt and transmission of data to proceed independently. By these means the control system response time is kept very short, even when the data collection rate is very high. Another advantage of this system architecture is that all major items, with the exception of the ILC boards, are available commercially. The ILC boards were designed in-house, and then loaded with commercially available components.

Acknowledgment

For the linac design, H. Hoag and R. Miller of SLAC have made valuable contributions.

References

[1] 1-2 GeV Synchrotron Radiation Source Conceptual Design Report, Lawrence Berkeley Laboratory PUB-5172, June 1986.

[2] Report of the Workshop on an Advanced Soft X-Ray and Ultraviolet Synchrotron Source, LBL PUB-5154, Dec. 1985.

[3] A. Jackson, LBL-22193, Mar. 1987, to be pub. in the proceedings of the 1987 Particle Accelerator Conference.

[4] A. Jackson and H. Nishimura, LBL-22194, ibid.

[5] A.W. Chao and J. Gareyte, SLAC pub. PEP-224, Dec. 1976.

[6] M.S. Zisman, S. Chattopadhyay and J.J. Bisognano, LBL-21270, Dec. 1986.

[7] S. Sakanaka, M. Izawa, H. Kobayakawa, and M. Kobayashi, NIM A256 (1987) 184.

[8] M.B. James, J.E. Clendenin, S.D. Ecklund, R.H. Miller, J.C. Sheppard, C.K. Sinclair and J. Sodja, IEEE Trans. Nucl. Sci. NS-30, No.4 (1983) 2992.

[9] F. Selph, A. Jackson and M.S. Zisman, LBL-22191, Mar. 1987, to be pub. in proc. of the 1987 Particle Accelerator Conference.

[10] M. Nakamura and J.A. Hinkson, IEEE Trans. Nucl. Sci. NS-32, No. 5 (1985) 1985.

FIGURE LEGENDS

Fig. 1. A plan view of the 1-2 GeV Synchrotron Radiation Source, showing the injection linac, booster, the storage ring lattice and the location of 5 insertion devices with beam lines, and two bending magnet beam lines.

Fig. 2. The storage ring enclosure in cross section, showing magnet, magnet stand, vacuum chamber and utilities.

Fig. 3. A plan view of the injector complex, showing in greater detail the 50 MeV linac, the 1.5 GeV booster, as well as the transfer lines.

Fig. 4. Spectral brightness as a function of energy for the four undulators and one wiggler for which parameters are given in Table III. For the undulators, the tuning range is shown for both the fundamental (solid lines) and the third harmonic (dashed lines). The dotted lines show corresponding curves for a magnet gap of 2.5 cm, the minimum that will be used during the commissioning period. The spectral brightness of bending magnet beams is also shown.

Fig. 5. Spectral flux as a function of energy for the four undulators and one wiggler of Table III, and for a bending magnet. The solid lines are for fundamental, and the dashed lines for third harmonic radiation. For undulators and wiggler a 5 mrad collection angle is assumed.

Fig. 6. Average coherent power as a function of energy for the four undulators and one wiggler of Table III. The K and L shell energies of several elements are also indicated.

Fig. 7. Plan view of one sector of the storage ring, showing the port at zero degrees for the beams emanating from an insertion device, and four ports for beams emanating from bending magnets.

Fig. 8. Plan of the storage ring magnet lattice for one sector, with three gradient bending magnets (B), Quadrupoles that control betatron functions in the long straight sections (QF and QD), quadrupoles that control dispersion in the arcs (QFA), and sextupoles for controlling chromaticity (SD and SF).

Fig. 9. Lattice functions for one sector of the storage ring magnet structure. The functions β_x, β_y are related to betatron oscillation amplitude, D to the dispersion.

Fig. 10. Dynamic aperture, or the aperture within which the electron motion is stable in the storage ring. The solid line is the aperture resulting from the action of the chromaticity-correcting sextupoles, and the inner shaded band shows the effect of magnet nonlinearities resulting from fabrication tolerances.

Fig. 11. Bunch length as a function of current, in 11a, for one bunch, in 11b for 250 bunches. The solid line shows the bunch length expected if, as is likely, SPEAR scaling of impedance is found to hold for the storage ring vacuum chamber (see text). The dashed line shows the bunch length that would be expected if SPEAR scaling was ignored.

Fig. 12. Beam lifetime as a function of energy, for 1 bunch and for 250 bunches. See remarks on SPEAR scaling in text and in legend for Fig. 11.

Fig. 13. The results of three calculations showing the effectiveness of a gap in the storage ring beam in reducing ion trapping. B is the number of beam bunches. The beam parameters were taken as 1.22 mA per bunch, horizontal emittance 4×10^{-9} m-rad, and the ratio of vertical to horizontal emittance 0.1. In the case with no gap (B = 328), all ions with masses 50 and below are stable, i.e., could be trapped in the beam. With a gap introduced (B = 272, and B = 216), most ions are unstable, i.e., will not be trapped.

Fig. 14. A cross section through the storage ring bending magnet and vacuum chamber.

Fig. 15. A cross section through the storage ring quadrupole magnet, showing how the vacuum chamber is shaped locally to allow components (in this case, pole tips and coils) to be as close as possible to the beam.

Fig. 16. Cutaway view of the storage ring vacuum chamber, showing the antechamber which is separated from the the beam chamber by a slot, of width just sufficient to allow the synchrotron radiation to pass through. Radiation which is not to be used in a beam line strikes a watercooled photon stop. A vacuum pump is positioned below the stop, to efficiently remove the evolved gases.

Fig. 17. A diagram showing the relation of beam bunches and rf in the bunchers, linac and booster. A 2.5 ns pulse from the gun is compressed in the subharmonic buncher, then is further compressed in the S-band buncher and linac, before being injected into a booster rf bucket. Phase-locking of the rf systems insures that the beam energy spread is not increased by phase mismatch between the various systems.

Fig. 18. A detail of the storage ring vacuum chamber in cross section showing one of the 96 beam position monitors (BPMs). Expected accuracy of the BPM measurement is 30 microns.

Fig. 19. Block diagram of the control system. It is entirely microprocessor-based, and makes much use of parallel processing to achieve speedy response.

Table I

Summary of major storage ring parameters[a]

Nominal energy (GeV)	1.5
Maximum circulating current, multibunch (mA)	400
Maximum circulating current, single bunch (mA)	7.6
Natural horizontal emittance (πm-rad)[b]	4.08×10^{-9}
Bunch length (ps), (2σ) at maximum current	
Multibunch (ps)	28
Single bunch (ps)	47
Peak energy (GeV)	1.9
Beam lifetime, half-life	
Gas scattering[c] (hr)	10.5
Touschek, maximum current	
Multibunch (hr)	18.5
Single bunch (hr)	8.4
Filing time	
Multibunch, to 400 mA (min)	2.1
Single bunch, to 7.6 mA per bunch (s)	16
Circumference (m)	196.8
Orbital period (ns)	656.4
Harmonic number	328
Radio frequency (MHz)	499.654
Peak effective rf voltage (MV)	1.5
Number of superperiods	12
Insertion straight section length (m)	6.75
Length available for insertion device (m)	5.0
Bending field (T)	1.248
Injection energy (GeV)	1.5
Betatron tunes	
Horizontal	14.28
Vertical	8.18
Synchrotron tune	0.0082
Natural chromaticities	
Horizontal	-24.1
Vertical	-28.5
Beta functions at insertion symmetry points	
Horizontal (m)	11.0
Vertical (m)	4.0
Momentum compaction	1.43×10^{-3}
Damping times	
Horizontal (ms)	13.1
Vertical (ms)	17.6
Longitudinal (ms)	10.7
Number of sextupole families	2

[a]All parameters at nominal energy unless otherwise noted.
[b]Defined as $\varepsilon = \pi\sigma^2/\beta$, where σ is the rms beam half size and β the amplitude function.
[c]10-mm vertical gap, 1 n Torr N_2

Table II

Performance goals established by potential Light Source users.

Beam energy, nominal (GeV)	1.5
Energy range (GeV)	0.75-1.9
Average current (mA)	400
Horizontal emittance, rms (πm-rad)	$< 10^{-8}$
Number of straight sections	12
Straight section length	
for insertion devices (m)	6
Bunch length, 2σ (ps)	20-50
Beam lifetime (hr)	> 6
High position and angular stability	
Minimum longitudinal jitter	

Table III

Parameters for the initial complement of insertion devices chosen for the Light Source

Name	Period (cm)	No. of periods	Photon energy range (eV)[a]	Critical energy (keV)
Undulators				
U20.0	20.0	23	0.5-95 [1.5-285]	-
U9.0	9.0	53	5-211 [15-633]	-
U5.0	5.0	98	50-380 [150-1140]	-
U3.65	3.65	134	183-550 [550-1650]	-
Wiggler				
W13.6	13.6	16	-	3.1

[a] The photon energy range of the fundamental and the third harmonic (shown in brackets) as K decreases from its maximum value to 0.5.

Table IV

Performance Requirements of Injector

ELECTRON GUN		
Single bunch mode		
Current	[A]	2.4
Pulse length	[ns]	2.5
Multibunch mode		
Current	[A]	1.0
Pulse length	[ns]	100
LINAC		
Energy	[MeV]	50
Repetition rate (max.)	[Hz]	10
Radiofrequency	[MHz]	2997.924
Single bunch mode		
Intensity		1.3×10^{10}
Bunch length (rms)	[ps]	15
Multi-bunch mode		
Average current	[mA]	125
Pulse length	[ns]	100
Emittance (rms)*	[πm-rad]	1.1×10^{-6}
Momentum spread (rms)	[%]	1.0
BOOSTER RING		
Injection energy	[MeV]	50
Nominal peak energy	[GeV]	1.5
Cycle rate	[Hz]	1
Single bunch mode		
Circulating current	[mA]	3.2
No. of stored electrons		5.0×10^{9}
Multibunch mode		
Circulating current	[mA]	20
No. of stored electrons		3.2×10^{10}
Beam properties at 1.5 GeV		
Natural rms emittance	[πm-rad]	1.45×10^{-7}
Energy spread, rms		6.3×10^{-4}
Bunch length, rms	[mm]	30.5

Table V

Intensities and Transmission for Electrons[a)]

	SINGLE BUNCH MODE		MULTI-BUNCH MODE	
	I (A)	N_e (10^{10})	I (mA)	N_e (10^{10})
Gun current	2.4	3.7	1000	26.6
Subharmonic buncher exit	-	2.6	292	18.6
S-band buncher exit	-	1.9	218	13.9
Linac exit	140	1.3	147	9.3
Accepted into booster	3.2	0.5	23	3.7
Extracted from booster	2.6	0.4	18	3.0
Storage ring accepted	0.5	0.2	3.4	1.5

a) Current values given are peak values for the gun and linac, and average values for the booster and storage ring.

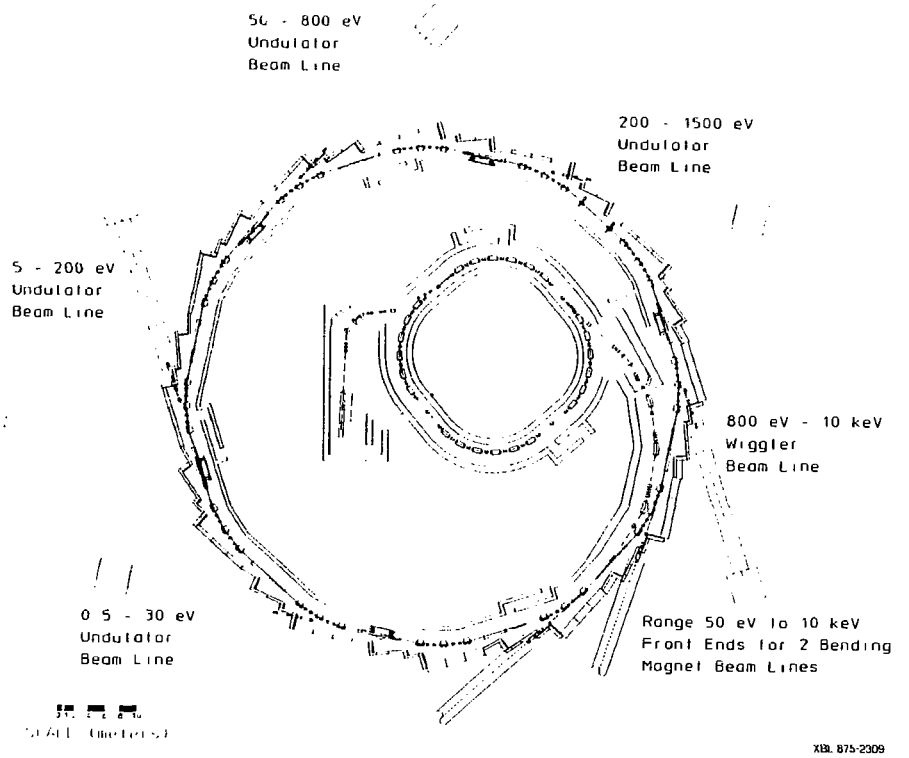
50 - 800 eV
Undulator
Beam Line
200 - 1500 eV
Undulator
Beam Line
5 - 200 eV
Undulator
Beam Line
800 eV - 10 keV
Wiggler
Beam Line
0.5 - 30 eV
Undulator
Beam Line
Range 50 eV to 10 keV
Front Ends for 2 Bending
Magnet Beam Lines
XBL 875-2309

Fig. 1

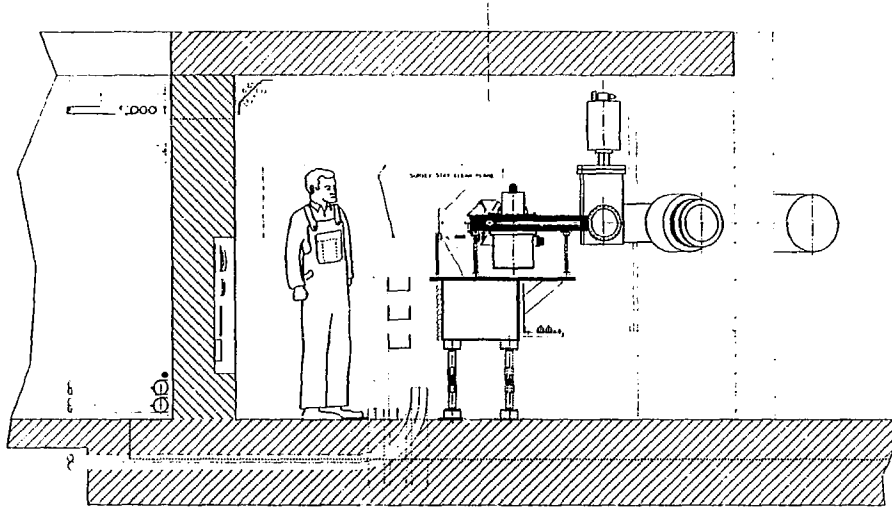

ALS STORAGE RING CROSS SECTION

XBL 875-2310

Fig. 2

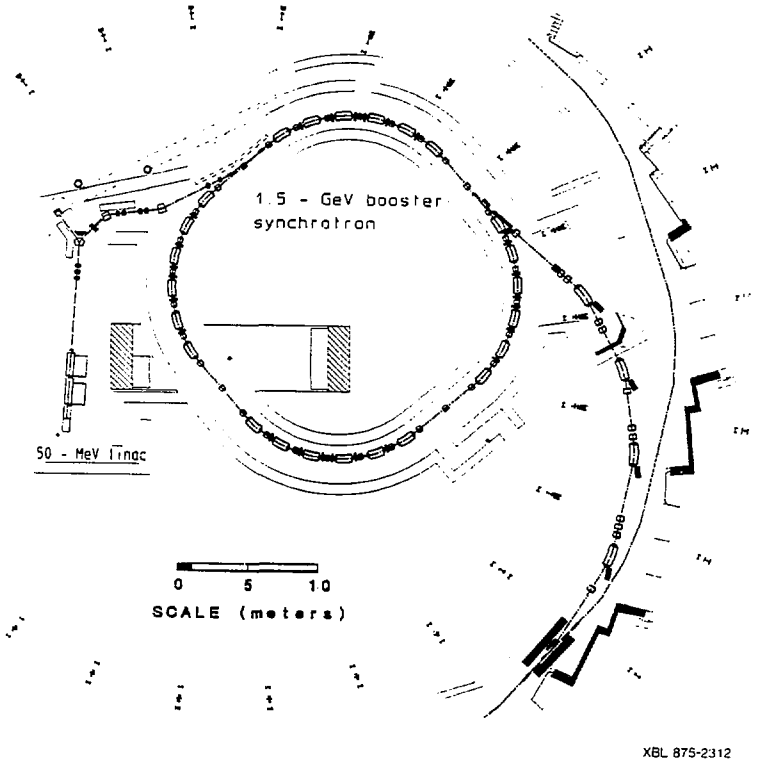
1.5 - GeV booster
synchrotron
50 - MeV Linac
0 5 10
SCALE (meters)
XBL 875-2312

Fig. 3

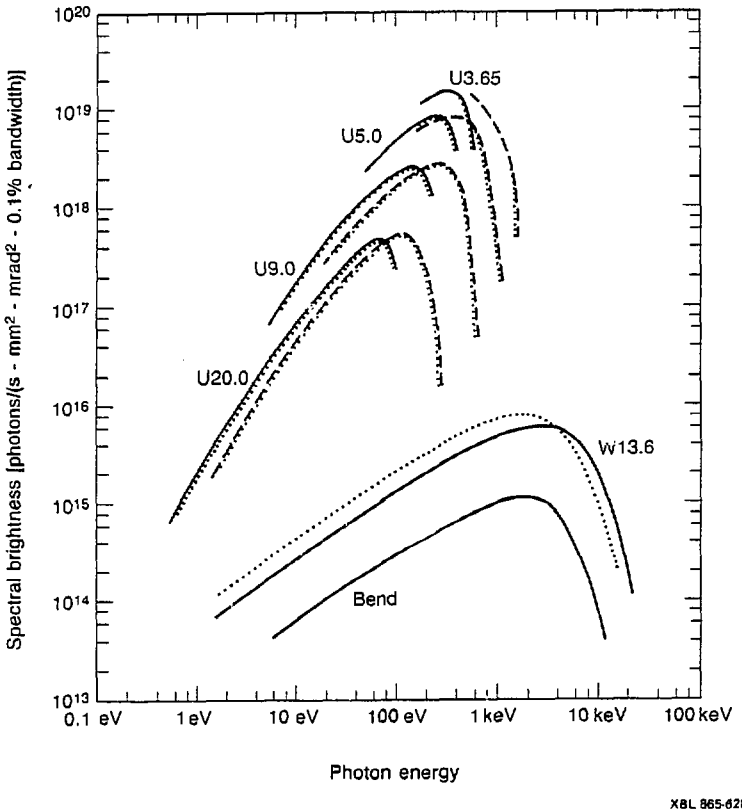
Spectral brightness [photons/(s - mm² - mrad² - 0.1% bandwidth)]
10²⁰
10¹⁹
10¹⁸
10¹⁷
10¹⁶
10¹⁵
10¹⁴
10¹³
U3.65
U5.0
U9.0
U20.0
W13.6
Bend
0.1 eV
1 eV
10 eV
100 eV
1 keV
10 keV
100 keV
Photon energy
X8L 865-6281

Fig. 4

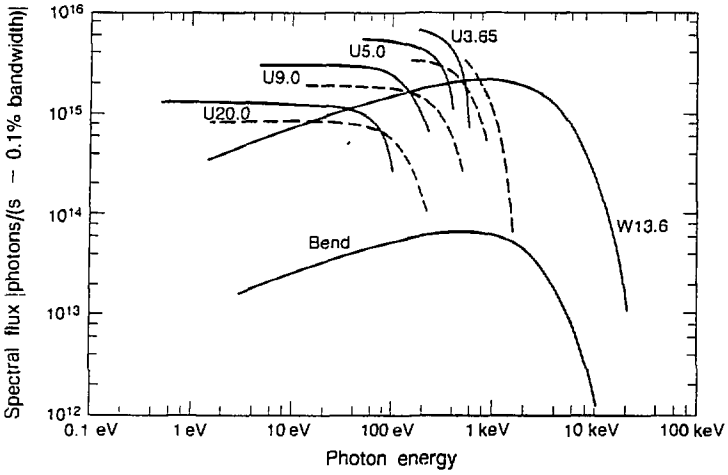

- For undulators, solid lines are the fundamental and dashed lines are the third harmonic radiation
- For wigglers and bending magnets, a 5 m-rad horizontal collection angle is assumed.
- E_e = 1.5 GeV, I = 400 mA, $\epsilon_x = 4\times10^{-9}$ m-rad, $\epsilon_y = 4\times10^{-10}$ m-rad

XBL 867-9462A

Fig. 5

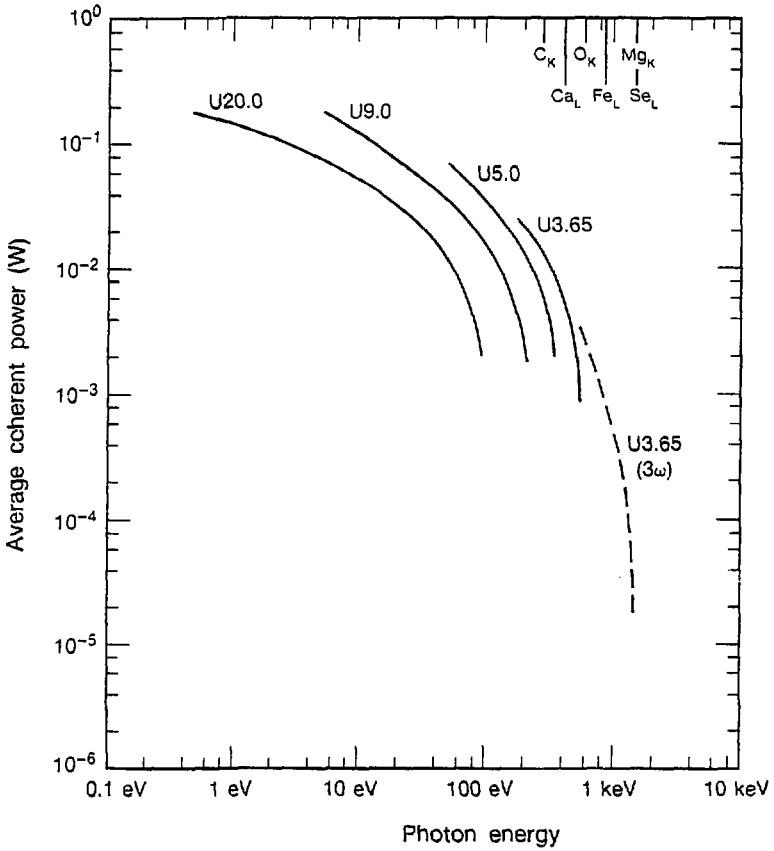

XBL 869-9823

Fig. 6

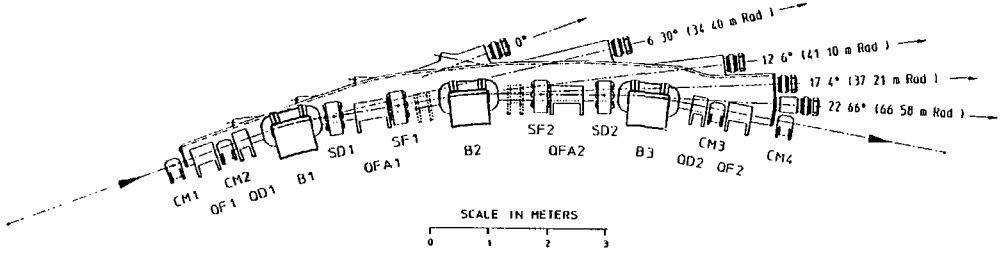
0°
6 30° (34 40 m Rad)
12 6° (41 10 m Rad)
17 4° (37 21 m Rad)
22 66° (66 58 m Rad)
CM1
CM2
QF1
QD1
B1
SD1
SF1
QFA1
B2
SF2
QFA2
SD2
B3
CM3
QD2
QF2
CM4
SCALE IN METERS
0
1
2
3
XBL 875-2313

Fig. 7

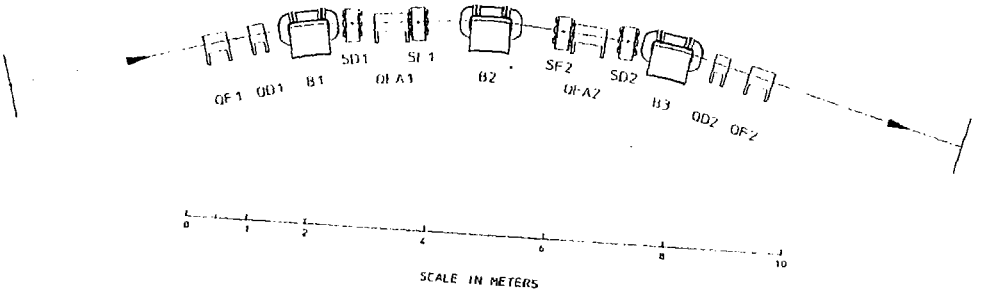

XBL 876-2643

Fig. 8

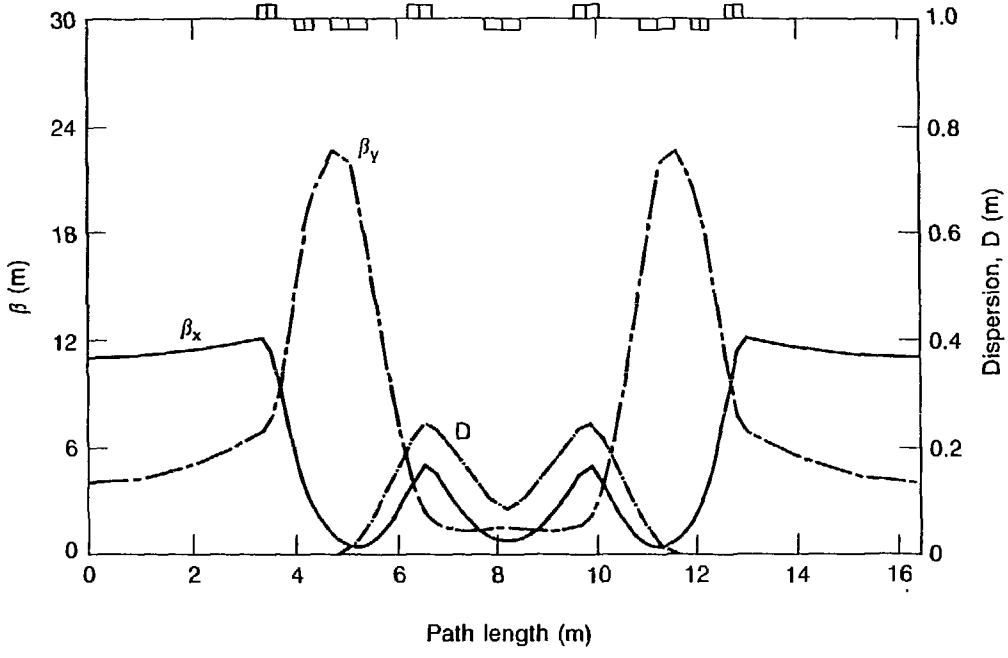

XBL 865-6248

Fig. 9

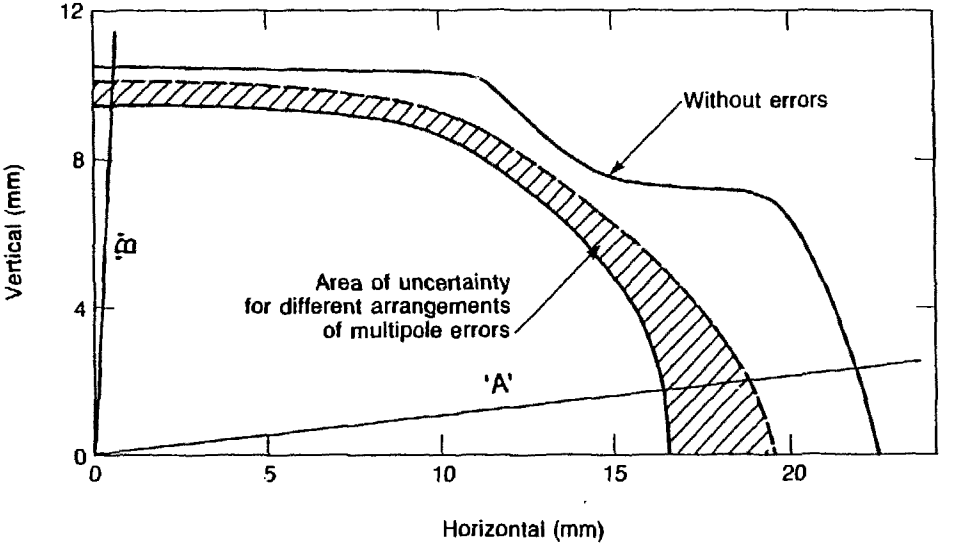
12
8
4
0
0
5
10
15
20
Vertical (mm)
Horizontal (mm)
Without errors
Area of uncertainty
for different arrangements
of multipole errors
'A'
XBL 865-6256

Fig. 10

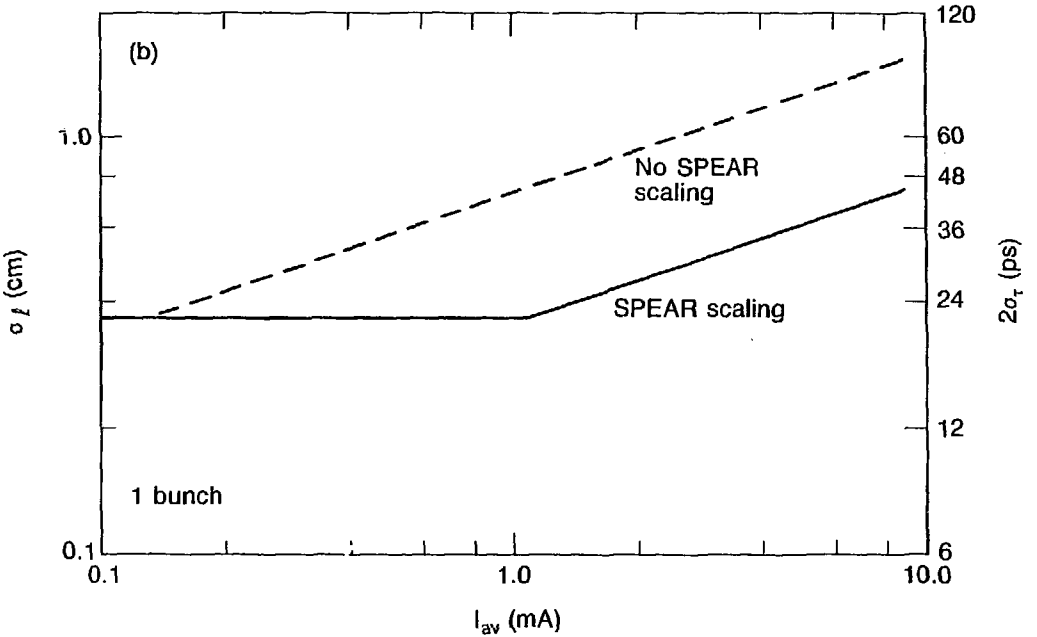

XBL 865-6235

Fig. 11(a)

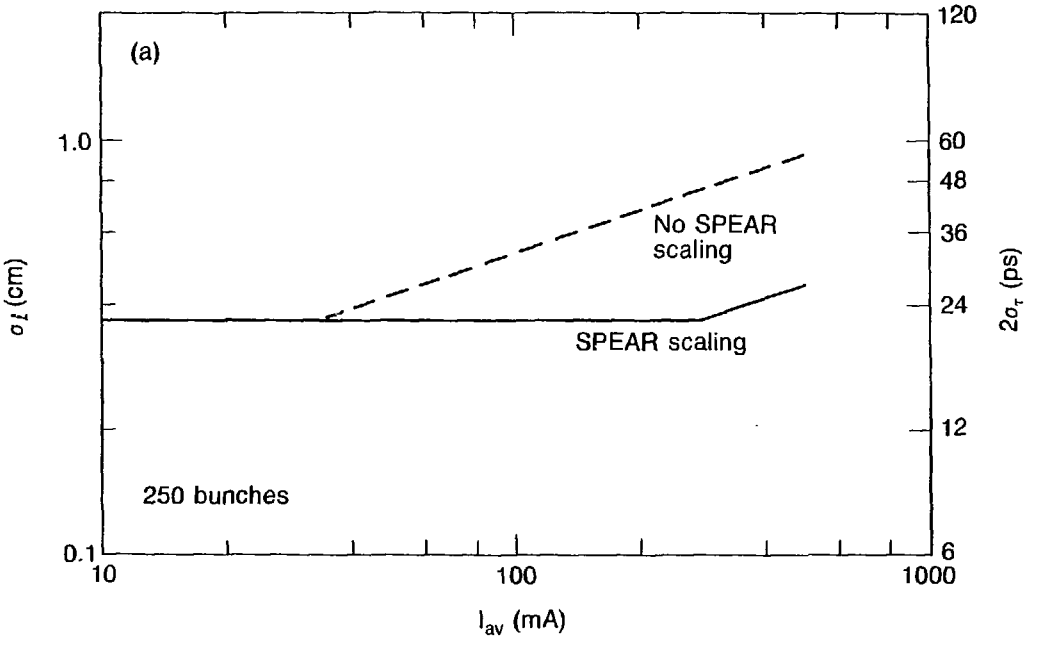

XBL 865-6234

Fig. 11(b)

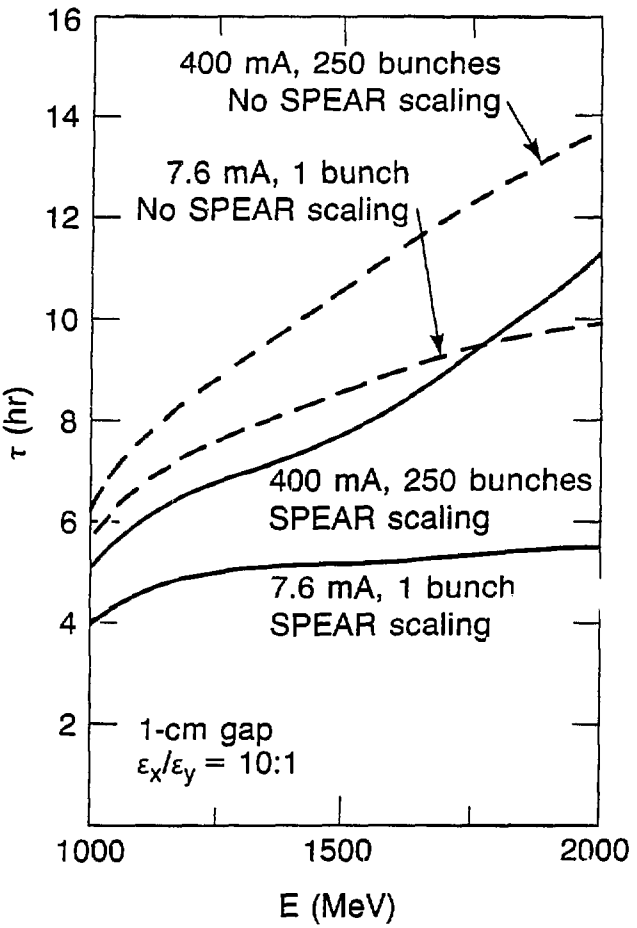

XBL 865-6224

Fig. 12

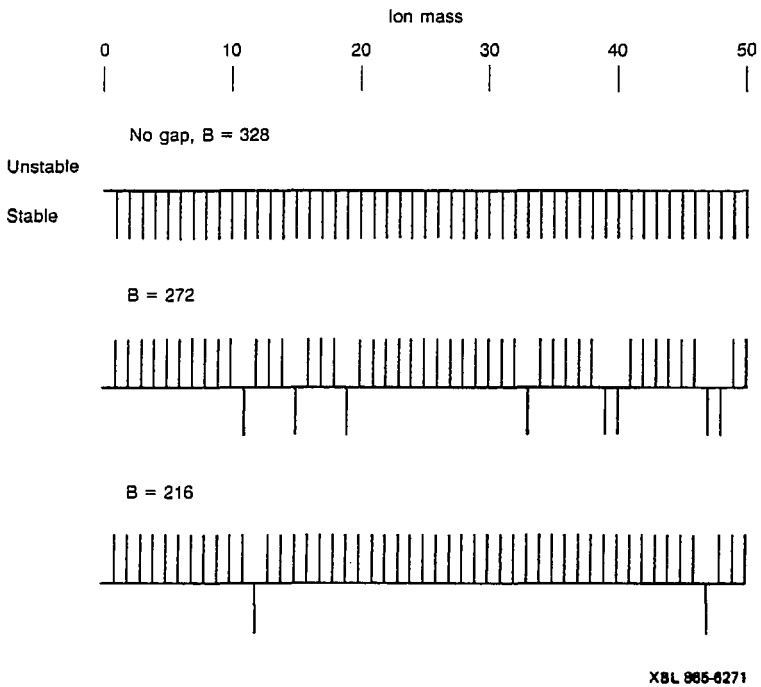
Ion mass
0
10
20
30
40
50
No gap, B = 328
Unstable
Stable
B = 272
B = 216
XBL 865-6271

Fig. 13

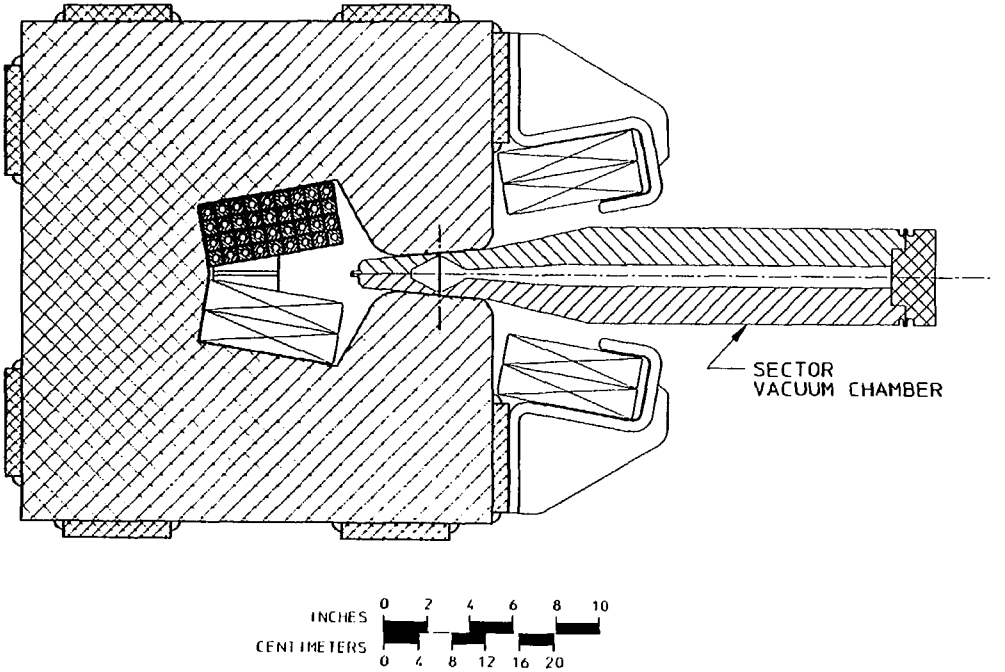

XBL 865-2037 A

Fig. 14

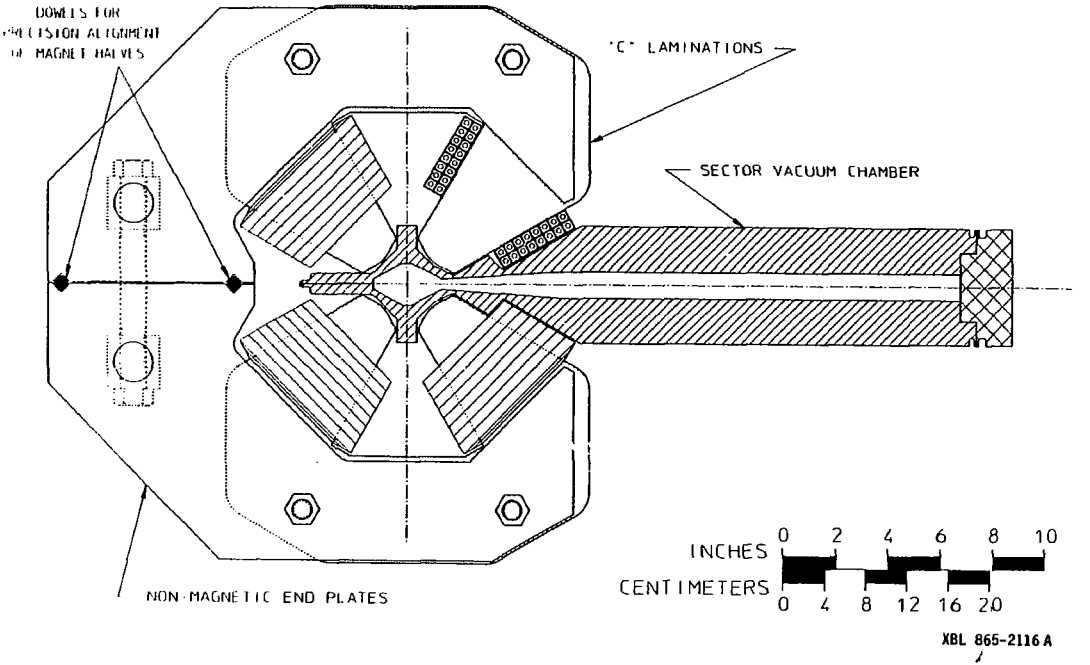
DOWELS FOR
PRECISION ALIGNMENT
OF MAGNET HALVES
"C" LAMINATIONS
SECTOR VACUUM CHAMBER
NON-MAGNETIC END PLATES
INCHES 0 2 4 6 8 10
CENTIMETERS 0 4 8 12 16 20
XBL 865-2116 A

Fig. 15

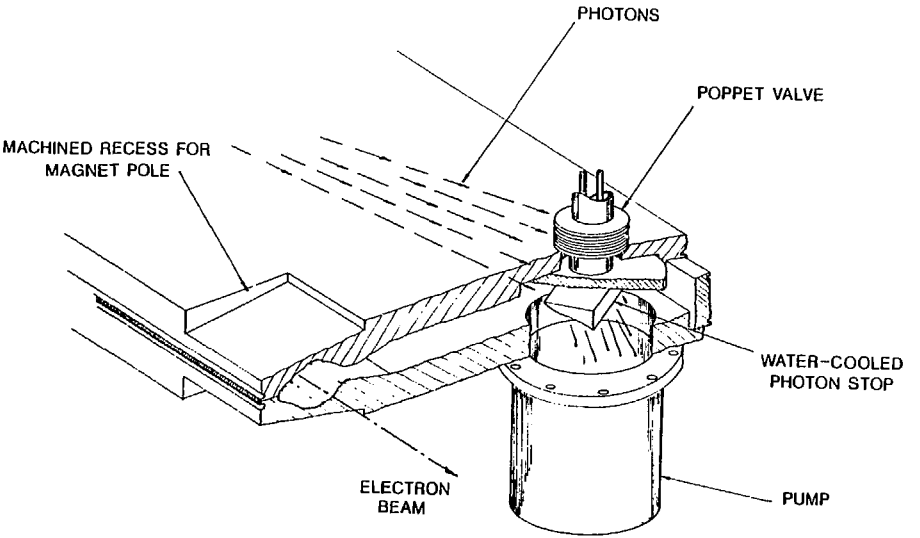

XBL 865-2028

Fig. 16

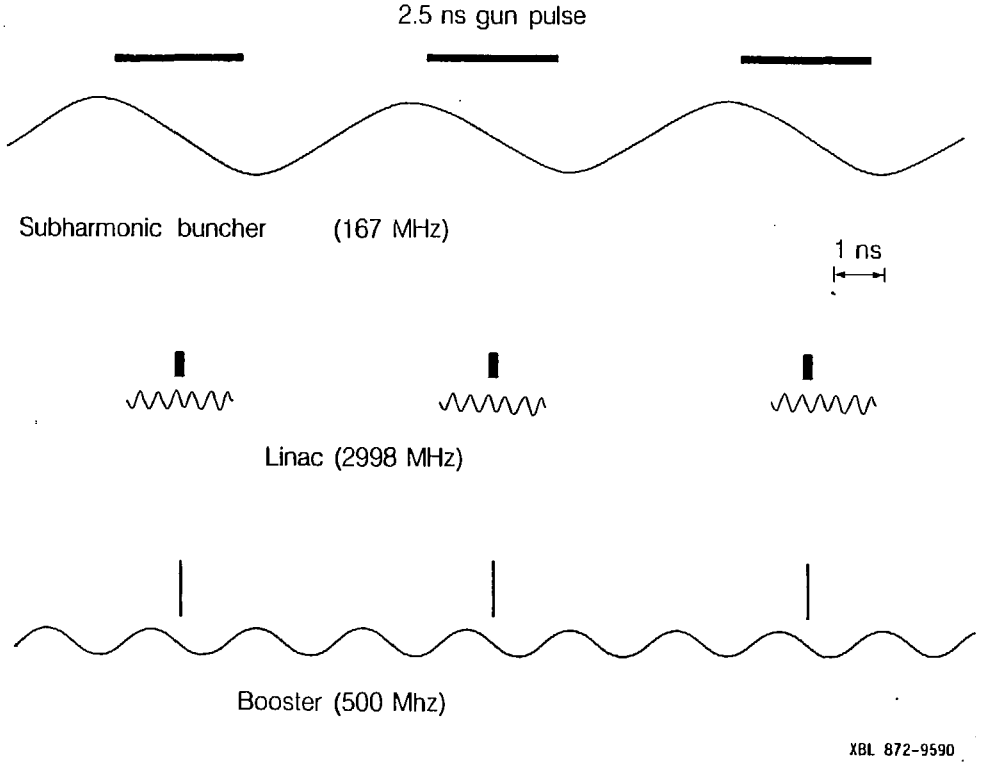
2.5 ns gun pulse
Subharmonic buncher (167 MHz)
1 ns
Linac (2998 MHz)
Booster (500 Mhz)
XBL 872-9590

Fig. 17

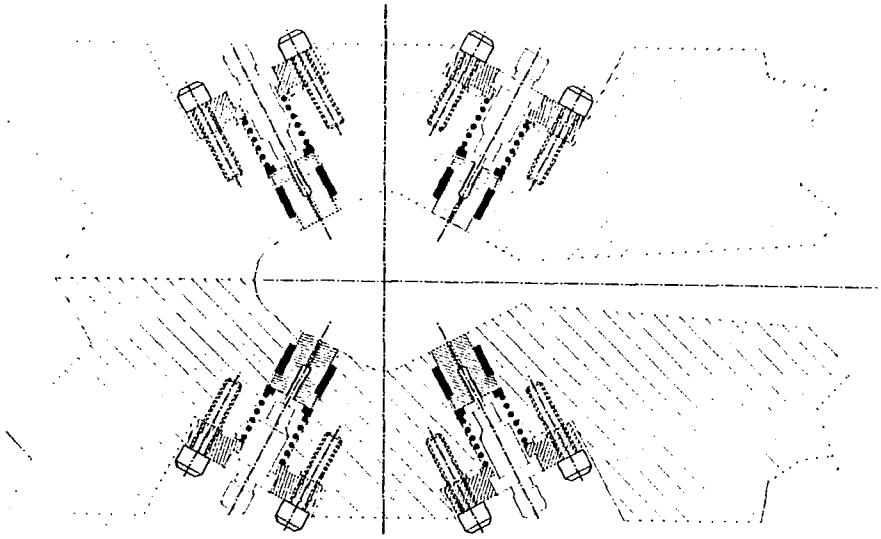
BEAM POSITION MONITOR
CROSS SECTION
0
1
2
3
4
SCALE IN INCHES
XBL 875-2311

Fig. 18

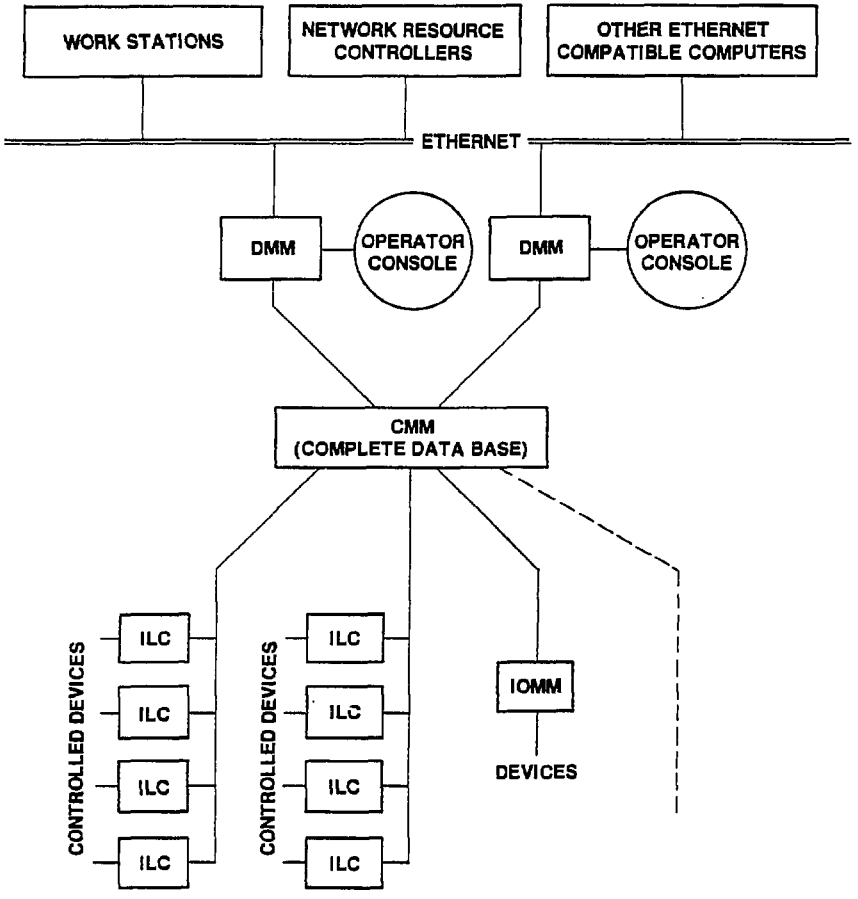

ALS CONTROL SYSTEM

XBL 8211-7403

Fig. 19